AD-A181 859   FLUORESCENCE AT A SURFACE(U) STATE UNIV OF NEW YORK AT   1/1
               BUFFALO DEPT OF CHEMISTRY H F ARNOLDUS ET AL JUN 87
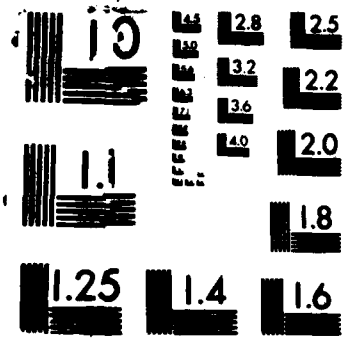   UBUFFALO/DC/87/TR-40 N00014-86-K-0043

UNCLASSIFIED   F/G 7/4   NL

DTIC FILE COPY

(12)

AD-A181 859

OFFICE OF NAVAL RESEARCH

Contract N00014-86-K-0043

R & T Code 413f0001-01

TECHNICAL REPORT No. 40

Fluorescence at a Surface

by

Henk F. Arnoldus, P. T. Leung and Thomas F. George
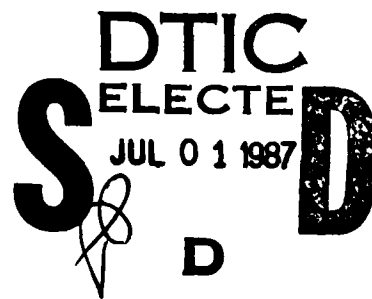
Prepared for Publication

in

Soviet Journal of Quantum Electronics

DTIC
SELECTED
JUL 0 1 1987
D

Departments of Chemistry and Physics
State University of New York at Buffalo
Buffalo, New York 14260

June 1987

87   6 30 080

REPORT DOCUMENTATION PAGE

1a. REPORT SECURITY CLASSIFICATION Unclassified		1b. RESTRICTIVE MARKINGS		
2a. SECURITY CLASSIFICATION AUTHORITY		3. DISTRIBUTION/AVAILABILITY OF REPORT Approved for public release; distribution unlimited		
2b. DECLASSIFICATION/DOWNGRADING SCHEDULE				
4. PERFORMING ORGANIZATION REPORT NUMBER(S) UBUFFALO/DC/87/TR-40		5. MONITORING ORGANIZATION REPORT NUMBER(S)		
6a. NAME OF PERFORMING ORGANIZATION Depts. Chemistry & Physics State University of New York	6b. OFFICE SYMBOL (If applicable)	7a. NAME OF MONITORING ORGANIZATION		
6c. ADDRESS (City, State and ZIP Code) Fronczak Hall, Amherst Campus Buffalo, New York 14260		7b. ADDRESS (City, State and ZIP Code) Chemistry Program 800 N. Quincy Street Arlington, Virginia 22217		
8a. NAME OF FUNDING/SPONSORING ORGANIZATION Office of Naval Research	8b. OFFICE SYMBOL (If applicable)	9. PROCUREMENT INSTRUMENT IDENTIFICATION NUMBER Contract N00014-86-K-0043		

8c. ADDRESS (City, State and ZIP Code) Chemistry Program 800 N. Quincy Street Arlington, Virginia 22217	10. SOURCE OF FUNDING NOS.			
	PROGRAM ELEMENT NO.	PROJECT NO.	TASK NO.	WORK UNIT NO.

11. TITLE
Fluorescence at a Surface

12. PERSONAL AUTHOR(S) Henk F. Arnoldus, P. T. Leung and Thomas F. George

13a. TYPE OF REPORT	13b. TIME COVERED FROM _____ TO _____	14. DATE OF REPORT (Yr., Mo., Day) June 1987	15. PAGE COUNT 22

16. SUPPLEMENTARY NOTATION
Prepared for Publication in the Soviet Journal of Quantum Electronics

17.	COSATI CODES		18. SUBJECT TERMS (Continue on reverse if necessary and identify by block number)
FIELD	GROUP	SUB. GR.	FLOURESCENCE MOLECULE NEAR SURFACE
			ATOM NEAR SURFACE SURFACE PLASMON
			CLASSICAL PHASE SHIFT SURFACE ROUGHNESS

19. ABSTRACT (Continue on reverse if necessary and identify by block number)

Fluorescence emitted by an atom near a metal surface and the coupling of the surface plasmon field of a dielectric substrate to a molecular electronic transition are studied. Explicit expressions for the atomic and molecular lifetimes are derived. It is shown how the (classical) phase shift of a plane wave upon reflection at the surface is responsible for the alteration of atomic lifetimes. Subsequently, it is demonstrated that the dipole direction of an atom can be fixed by illumination of the system with a polarized light source. For molecular transitions, the surface-plasmon and the surface-roughness contribution to the decay constants are included. In a comparison between the image theory and the energy-transfer theory, it appears that the former can be rather inaccurate for large molecule-surface separations or a highly-conducting substrate.

20. DISTRIBUTION/AVAILABILITY OF ABSTRACT UNCLASSIFIED/UNLIMITED ☒ SAME AS RPT. ☒ DTIC USERS ☐	21. ABSTRACT SECURITY CLASSIFICATION Unclassified	
22a. NAME OF RESPONSIBLE INDIVIDUAL Dr. David L. Nelson	22b. TELEPHONE NUMBER (Include Area Code) (202) 696-4410	22c. OFFICE SYMBOL

FLUORESCENCE AT A SURFACE

Henk F. Arnoldus, P. T. Leung and Thomas F. George
Departments of Physics & Astronomy and Chemistry
239 Fronczak Hall
State University of New York at Buffalo
Buffalo, New York 14260 USA

Abstract

Fluorescence emitted by an atom near a metal surface and the coupling of the surface plasmon field of a dielectric substrate to a molecular electronic transition are studied. Explicit expressions for the atomic and molecular lifetimes are derived. It is shown how the (classical) phase shift of a plane wave upon reflection at the surface is responsible for the alteration of atomic lifetimes. Subsequently, it is demonstrated that the dipole direction of an atom can be fixed by illumination of the system with a polarized light source. For molecular transitions, the surface-plasmon and the surface-roughness contribution to the decay constants are included. In a comparison between the image theory and the energy-transfer theory, it appears that the former can be rather inaccurate for large molecule-surface separations or a highly-conducting substrate.

Keywords: fluorescence, lifetimes, surface, photon correlations

I. INTRODUCTION

An atom in empty space decays spontaneously (accompanied by the emission of a fluorescent photon), with a certain lifetime, which is brought about by the coupling of the atomic (transition) dipole moment to the travelling plane wave modes of the electromagnetic vacuum field. Early attempts to comprehend the process of spontaneous emission concentrated on the prediction of the Einstein A_o coefficient, which equals the inverse lifetime of an excited state, and it was one of the first victories of quantum mechanics by Dirac in 1927 to establish unambiguously its value as

$$A_o = \frac{\omega^3}{3\pi\epsilon_o \hbar c^3} \cdot \frac{|<j_e\|\mu\|j_g>|^2}{2j_e+1} \; . \tag{1.1}$$

Here, $<j_e\|\mu\|j_g>$ is the reduced matrix element of the atomic dipole operator $\underline{\mu}$ between an excited level $|j_e m_e>$ and the ground level $|j_g m_g>$, which have a level separation $\hbar\omega$. Result (1.1) follows from the Golden Rule and is an essentially quantum mechanical expression (because of the appearance of $\hbar$).

Earlier this year[1,2] it was demonstrated for the first time that it is practically feasible to alter atomic lifetimes for optical transitions through a (semi) confinement of the atom. This was brought about by passing an atomic beam through a set of parallel mirrors or a confocal resonator. In this paper we report recent developments in the theoretical understanding of atomic fluorescence near a metal surface.

Another technique to change the lifetime of an electronic transition pertains to the deposition of a molecular monolayer on a dielectric bulk material. Then the separation between the optically-active compound and the passive substrate can be extremely small, which implies that the lifetime

modification is brought about mainly by coupling to the short-range evanescent plasmon field. Since the decaying system is so close to the surface, it becomes inevitable to take the details of the surface structure (roughness) into consideration.

II. ATOMIC DECAY

The plane $z = 0$ separates the vacuum $z > 0$ from a substrate in $z < 0$, which is assumed to be fairly represented by its dielectric constant $\epsilon(\omega)$. An atom is positioned on the z-axis at $d\underset{\sim}{e}_z$ with $d > 0$. Since every radiation field in the region above the surface can be expanded in plane waves, it should be possible to express any surface effect in an observable quantity in terms of the plane-wave Fresnel reflection coefficients. These are for s(urface) and p(lane) polarized waves

$$R_s(\omega,u) = \frac{\sqrt{\epsilon(\omega)-1+u^2} - u}{\sqrt{\epsilon(\omega)-1+u^2} + u} \quad , \tag{2.1}$$

$$R_p(\omega,u) = \frac{u\epsilon(\omega) - \sqrt{\epsilon(\omega)-1+u^2}}{u\epsilon(\omega) + \sqrt{\epsilon(\omega)-1+u^2}} \quad , \tag{2.2}$$

where u signifies the cosine of the angle of incidence. Then the mode expansion of the electric field in the region $z > 0$, becomes

$$\underset{\sim}{E}(\underset{\sim}{r},t) = \sum_{\underset{\sim}{k}\sigma} \sqrt{\frac{\hbar\omega_{\underset{\sim}{k}}}{2\epsilon_o}} \; a_{\underset{\sim}{k}\sigma}(t) \; \underset{\sim}{F}_{\underset{\sim}{k}\sigma}(\underset{\sim}{r}) \quad , \tag{2.3}$$

with $\underset{\sim}{F}_{\underset{\sim}{k}\sigma}(\underset{\sim}{r})$ the sum of an incident and a reflected wave, and normalized in such a

way that every photon carries an energy $\hbar\omega$.[3] The equation of motion for the density operator of the system reads

$$i\hbar\frac{d\rho}{dt} = [H_a + H_r + H_i , \rho] ,$$

(2.4)

where a, r and i indicate atomic, radiation and interaction, respectively.

Transparent interpretations can be obtained if we restrict our attention to (idealized) metals, defined by $\epsilon(\omega) < 0$. From Eqs. (2.1) and (2.2) it then follows that

$$|R_\sigma(\omega,u)| = 1 ,$$

(2.5)

and hence the metal is perfectly reflecting. Then we can write

$$R_\sigma(\omega,u) = e^{2i\phi_\sigma(\omega,u)} ,$$

(2.6)

and the real-valued phase shifts ϕ_σ for s and p waves follow directly from a comparison with Eqs. (2.1) and (2.2). For a perfectly-conducting metal we have $\phi_\sigma \equiv 0$.

In writing $|j_e m_e\rangle$ for a magnetic substate of the upper level, we implicitly refer to a direction in configuration space, e.g., the quantization axis. In our geometry it is most advantageous to take this direction to coincide with the normal to the surface. With this convention the atomic wave functions are unambiguously defined. Then it is a standard procedure[4] to eliminate the explicit occurrence of the radiation field from the equation of motion (2.4), which yields the Einstein coefficients A_{m_e} for the decay of $|j_e m_e\rangle$. We find

$$A_{m_e} = A_o \sum_{m_g \tau} b_\tau(d)(j_g m_g 1\tau | j_e m_e)^2 \quad , \tag{2.7}$$

where τ assumes the values -1, 0, 1, corresponding to the three possible helicities of a fluorescent photon. The parameter functions $b_\tau(d)$ embody the surface modifications to the relaxation constants, and they are explicitly

$$b_{\parallel}(d) = b_{\pm 1}(d) = 1 - \frac{3}{4} \int_0^1 du \cos(2(\omega du/c + \phi_s(\omega,u)))$$

$$- \frac{3}{4} \int_0^1 du \, u^2 \cos(2(\omega du/c + \phi_p(\omega,u))) \quad , \tag{2.8}$$

$$b_{\perp}(d) = b_0(d) = 1 + \frac{3}{2} \int_0^1 du \, (1-u^2)\cos(2(\omega du/c + \phi_p(\omega,u))) \quad . \tag{2.9}$$

Expressions (2.8) and (2.9) are identical to those obtained by Philpott,[6] in a different way.

In the limit $d \to \infty$, we find $b_{\parallel} = b_{\perp} = 1$ and $A_{m_e} = A_o$, which implies that the atom behaves as an atom in free space (no surface), and that the lifetime of the state $|j_e m_e\rangle$ becomes independent of m_e. Conversely, due to the presence of the surface, every excited state has a different relaxation constant A_{m_e}. The relation $A_{m_e} = A_0$ for an atom in empty space reflects the isotropy of spontaneous emission, or, the spherical symmetry of the system. In the vicinity of a boundary, this symmetry is destroyed, which gives every state $|j_e m_e\rangle$ a different lifetime. From Eq. (2.7) we see that

$$A_{m_e} = A_{-m_e} \quad , \tag{2.10}$$

which displays the remaining cylindrical symmetry for rotaions about the z-axis.[7]

By summing Eq. (2.7) over the magnetic quantum numbers m_e, we obtain the sum rule

$$\frac{1}{2j_e+1} \sum_{m_e} A_{m_e} = \frac{1}{3}A_\perp + \frac{2}{3}A_\parallel \quad , \tag{2.11}$$

with $A_\perp = A_0 b_\perp$ and $A_\parallel = A_0 b_\parallel$. Here, the left-hand side is the average value of A_{m_e} over the different substates, because there are $2j_e + 1$ excited states $|j_e m_e\rangle$ for a given j_e. If the population of the excited state is randomly distributed over the various substates, with no coherence between the states, then the atom will effectively decay with the average of A_{m_e}. In this respect the result (2.11) is a quantum mechanical justification for a randomization of the dipole direction, which is commonly applied in semiclassical theories of relaxation near an interface. For excitation with a polarized light source this procedure is not correct, as we shall show in due course.

Another interesting feature is the dependence of the lifetimes on the distance d between atom and surface. From Eqs. (2.8) and (2.9) we see that $b_\parallel(d)$ and $b_\perp(d)$ are determined by a superposition of waves with a different value of u, where u is the cosine of the angle of incidence. Properties of the reflecting medium are accounted for by the phase shifts $\phi_\sigma(\omega,u)$. From this interpretation it follows that the d dependence of A_{m_e} is brought about by simple interference of plane waves, which is a pure classical effect. The relevance of the phase shift is most easily demonstrated by considering the limit $d \to 0$. In the case of a perfect conductor we then find

$$b_\parallel(0) = 0 \quad , \quad b_\perp(0) = 2 \quad , \tag{2.12}$$

whereas the limit $\epsilon \to 0$ yields

$$b_{\parallel}(0) = 1 \quad , \quad b_{\perp}(0) = 0 \quad . \tag{2.13}$$

For a perfectly-conducting solid the inverse lifetime of a parallel dipole is zero, but if the conductivity becomes smaller, it is the inverse lifetime of a perpendicular dipole which vanishes. This reversal of behavior of parallel and perpendicular dipoles as a function of the conductivity illustrates the dramatic effect that a phase change upon reflection of a plane wave can have on the optical properties of an atom, which experiences these plane-wave fields. Figure 1 gives more details of the ϵ dependence of $b_{\parallel}(0)$ and $b_{\perp}(0)$.

III. FLUORESCENCE

Dynamical behavior of an atom in a radiation field can be studied experimentally by observation of the fluorescence. Information on various details, like lifetimes, is reflected in the different statistical properties of the emitted radiation. Therefore, we consider the (quantum) radiation field in more detail. In Eq. (2.3) we gave the general expression for the electric field $\underline{E}(\underline{r},t)$, and we notice that its time dependence only enters through the time dependence of the annihilation operator $a_{\underline{k}\sigma}(t)$. By definition, this Heisenberg operator obeys the time-evolution equation

$$i\hbar\frac{d}{dt}\, a_{\underline{k}\sigma}(t) = [a_{\underline{k}\sigma}(t) \, , \, H_a + H_r + H_i] \quad . \tag{3.1}$$

If we work out the commutator, differentiate the equation with respect to time and substitute the result in the second time derivative of Eq. (2.3), then it

follows that $\underline{E}(\underline{r},t)$ obeys the wave equation, with the dipole moment as source term.[8] We can solve this equation and make an asymptotic expansion for $r = |\underline{r}| \rightarrow \infty$, which finally yields the expression for the electric field in the radiation zone

$$\underline{E}(\underline{r},t) = \frac{\omega^2}{4\pi\epsilon_0 rc^2} \int_\sigma \underline{\epsilon}_{\underline{r}\sigma}(\underline{\epsilon}_{\underline{r}\sigma} \cdot \{\underline{\mu}(t-r/c)e^{-i\omega du/c}$$

$$+ \underline{\mu}'(t-r/c)e^{i(\omega du/c+2\phi_\sigma(\omega,u))} \}) + \text{h.c.} + \text{free field} \quad . \quad (3.2)$$

Here, the polarization vectors $\underline{\epsilon}_{\underline{r}\sigma}$ correspond to the plane waves which travel in the direction of observation $\underline{r}$, and u is now the cosine of the angle of observation (angle between $\underline{r}$ and the z-axis). The mirror dipole moment $\underline{\mu}'$ is defined as $\underline{\mu}' = \underline{\mu}_\perp - \underline{\mu}_\parallel$ in terms of the separation $\underline{\mu} = \underline{\mu}_\perp + \underline{\mu}_\parallel$ for the atomic dipole. Result (3.2) encompasses all spectral, temporal and polarization properties of the emitted photons, including their angular distribution. We notice that the surface-conductivity effect is incorporated by the phase shift ϕ_σ of the component with source $\underline{\mu}'$, which originates from the mirror dipole in $\underline{r} = -d\underline{e}_z$ below the surface.

IV. PHOTON CORRELATIONS

Recently[9] we advocated that in designing an experiment for the observation of surface-modified optical properties of atoms, one can greatly benefit from the polarization properties of the fluorescence, which are induced by the presence of the substrate. Especially the combination with state-selective excitation by an intense polarized laser beam, propagating in a well-defined direction, allows the construction of a geometrical configuration for which only a specific combination

of $A_\perp$ and $A_\parallel$ determines the statistical properties of the fluorescence. In order to illstrate the idea, we consider a $j_e = 1 \rightarrow j_g = 0$ transition. If we take the incident cw laser field to be linearly polarized and travelling in a direction parallel to the surface, then it follows from the dipole selection rules that only the state $|1,0\rangle$ will be populated. Alternatively, we can assume a circularly-polarized beam which is incident normal to the surface. In this case only one of the substates $|1,\pm 1\rangle$ will be occupied. Since $|1,0\rangle$ and $|1,\pm 1\rangle$ decay with an inverse lifetime equal to $A_\perp$ and $A_\parallel$ respectively, we can simply fix the dipole direction with our choice of external field.

Driving an atomic transition with a cw laser results in a time-independent fluorescent intensity I, and consequently the information contained in this quantity is minimal. Therefore, we consider the stationary two-photon correlation function f(t), which has the significance of the probability for the detection of a photon at time $t \geq 0$, after the detection of a photon at time zero, and irrespective of possible detections at other times (for instance in [0,t]). In general the function f(t) acquires the form

$$f(t) \propto \langle E^{(-)}(0)E^{(-)}(t)E^{(+)}(t)E^{(+)}(0)\rangle \quad , \tag{4.1}$$

where $E^{(+)}(t)$ is the projection of $\underline{E}^{(+)}(\underline{r},t)$ on the polarization direction of a polarizer. Evaluation of this expression is quite involved,[7] so here we shall merely quote the result. We find

$$f(t) = I\{1-e^{-3At/4}(\cos(\Omega t)+3A\sin(\Omega t)/4\Omega)\} \tag{4.2}$$

for a strong laser exactly on resonance with the transition frequency ω. Here, Ω denotes the Rabi frequency ($\Omega^2 \propto$ laser power). Surface-induced effects are

entirely incorporated in the Einstein coefficient A, which equals $A_\perp$ for the linearly-polarized case ($\Delta m = 0$), and $A_\parallel$ for a circularly-polarized laser ($\Delta m = \pm 1$). The advantage of a laser-driven atom and observation of the photon correlations is that the desired relaxation constant can simply be selected by an appropriate choice of external field.

V. MOLECULAR DECAY AT ROUGH SURFACES

In the previous sections perfect flatness of the surface has been assumed. However, there are many experiments with large admoleucles (e.g., pyrazine) in which roughness of the surface unavoidably exists.[10] Hence, in this section we shall summarize some of our recent work on molecular decay rates at rough metallic surfaces, where surface plasmon excitation has been found to play a dominant role.

To simplify the problem, we shall follow a classical phenomenological approach based on Maxwell's theory, which has been found to be adequate for molecule-surface distances (d) greater than a few Angstroms. Then the "quantum spreads" of both the surface and the molecule can be neglected.[11] Within this approach, the molecule is modeled as a point dipole (μ), satisfying the damped-oscillator equation of motion, driven by the surface field ($\underline{E}$). The induced decay rate obtained in this model can be expressed as[12-14]

$$A_F = A_o(1 + \frac{3}{2}\frac{q}{k^3}\,\mathrm{Im}G^F) \ , \tag{5.1}$$

$$A_R = A_o[1 + \frac{3}{2}\frac{q}{k^3}\,\mathrm{Im}(G^F+G^R)] \ , \tag{5.2}$$

where q is the quantum yield of the emitting state, $k = \omega/c$ equals the emission wave number, and the sub(super)scripts R, F and o stand for cases with a rough

surface, flat surface and free molecule respectively. The G-functions in Eqs. (5.1) and (5.2) are defined as the surface field acting on the molecule per unit dipole moment and as a function of the emission frequency

$$G(\omega) = \frac{E(\omega)}{\mu} \ . \tag{5.3}$$

Note that in writing Eq. (5.2) we have followed an approach which distinguishes between the contributions to the surface-induced decay rates from the flat boundary and from the roughness, respectively.[13,14]

The remaining task in this approach is to calculate the $G(\omega)$-functions. In general, there are two ways of doing this, namely, the image method and the energy-transfer theory. In the image theory (IT), one regards the surface field $E(\omega)$ as given by the image field, induced by the molecular dipole, which is obtained from solving the electrostatic Poisson equation. For example, in the case of a flat surface and μ located at $(0,0,d)$, oriented perpendicular to the surface, one obtains[14]

$$G_{IT}^{F}(\omega) = \frac{k^3}{4\bar{d}^3} \frac{\varepsilon-1}{\varepsilon+1} \ , \tag{5.4}$$

where $\bar{d} \equiv kd$ is the reduced distance and $\varepsilon(\omega) = \varepsilon_1(\omega) + i\varepsilon_2(\omega)$ is the complex bulk dielectric constant of the substrate material.

The other approach, energy-transfer theory (ET), is a more exact electrodynamical treatment in which one has to solve the full set of Maxwell's equations (or the Helmholtz wave eqution) by regarding the dipole emission as the source (incident) field, and by matching boundary conditions at the surface. Then $E(\omega)$ will be given by the reflected field from the surface, evaluated at the

molecular site. For the case of a flat surface, this problem has been solved by Chance, Prock and Silbey[12] (CPS) by applying the Sommerfeld theory for a radiating dipole antenna above the earth's surface. Thus for the above example the CPS theory gives

$$G_{ET}^{F}(\omega) = -k^3 \int_0^\infty du \, R_p(\omega, i\ell_1) \, e^{-2\ell_1 \bar{d}} \frac{u^3}{\ell_1} \, , \qquad (5.5)$$

where $\ell_1 = -i(1-u^2)^{\frac{1}{2}}$.

It is obvious from the above examples that IT is in general an approximate but much simpler approach than ET. It has been a wide belief[15] that in the short-distance or long-wavelength limit ($\bar{d}\ll1$), which holds for most experimental conditions ($d \leq 10^2$ Å and $\lambda \sim 10^3$ Å),[16] IT should be accurate enough to describe the phenomenon. Moreover, although both IT and ET are available for the case of flat surfaces, only IT is available so far in the literature when surface roughness cannot be neglected.[13,14]

In a recent analysis of the limit of IT, however, it was pointed out that the condition $d \ll \lambda$ is not sufficient to ensure IT to be valid.[17] The additional condition found for IT to hold is $d \ll \delta$, with δ being the skin depth of the substrate. In particular, for a highly-conducting substrate such as silver and for the above example, IT has been found to break down appreciably for $d \geq 0.01\lambda$. Roughly speaking, the physical origin for such a failure of IT stems from the fact that the Helmholtz wave equation in a conducting medium does not reduce to the static Poisson equation in the limit $\lambda \to \infty$, if the conductivity of the medium becomes infinite.

It is therefore necessary to develop a dynamical theory (ET) for a complete description of the decay rates of admolecules at rough surfaces. Recently, an attempt[18] in this direction was made by combining the CPS theory[12] and the

integral-equation formalism of Maxwell's equations for rough boundaries, established chiefly by Maradudin and Mills (MM)[19] and Agarwal.[20] Let us describe the roughness by a profile function $\zeta(x,y)$. The main idea of the MM theory is to regard ζ as a source for the homogeneous Hemholtz equation in the case of a perfectly-flat boundary. One is then able to obtain perturbative solutions in orders of ζ for the reflected field $\underline{E}(\omega)$, which is the relevant surface field for the calculation of the $G(\omega)$-functions. Then $\underline{E}(\omega)$ is expressible as a combination of the contributions from the flat boundary and the roughness as

$$\underline{E} = \underline{E}^F + \underline{E}^R \quad , \tag{5.6}$$

and to order ζ one obtains for the μ-th component of $\underline{E}^R$ [19]

$$E_\mu^R(\underline{r};\omega) = -\frac{k^2}{16\pi^3}[\epsilon(\omega)-1]\int d^2k_{\|}\, e^{i\underline{k}_{\|}\cdot\underline{r}_{\|}}\, \zeta(\underline{k}_{\|}-\underline{k}_{\|}^{(0)})$$

$$\times \int dz'\, d_{\mu\nu}(\underline{k}_{\|}\omega|zz')\delta(z')\, E_\nu^{(0)}(\underline{k}_{\|}^{(0)}\omega|z') \quad . \tag{5.7}$$

Here, $\underline{E}^{(0)}$ is the total field for a perfectly flat boundary, and ζ and $d_{\mu\nu}$ are the Fourier transforms of the profile function and the Green tensors, respectively, as given in Ref. 19. The evaluation of the δ functions for discontinuous fields across a boundary is understood to follow MM together with Agarwal's prescription.[19,20]

To illustrate this dynamical theory, we consider the simple case of a perpendicular dipole located at $(0,0,d)$ above a shallow sinusoidal grating. After application of the CPS theory for the calculation of $\underline{E}^{(0)}$, we obtain to lowest order in ζ

$$E_z^R(d;\omega) = -i\mu k^3 \frac{(\epsilon-1)}{4\pi^2} \int d^2 k_{\parallel} \; \hat{\zeta}(\underline{k}_{\parallel}) \frac{k_{\parallel}^2 e^{ik_2 d}}{k_1 - \epsilon k_2} \int_0^{\infty} du \; (1-R_p) \frac{u^3}{\ell_1} e^{-\ell_1 \bar{d}} \quad , \quad (5.8)$$

where

$$k_1 = -[\epsilon(\omega)k^2 - k_{\parallel}^2]^{\frac{1}{2}} \; ,$$

$$k_2 = \begin{cases} (k^2 - k_{\parallel}^2)^{\frac{1}{2}} \; , \; k^2 > k_{\parallel}^2 \\[12pt] i(k_{\parallel}^2 - k^2)^{\frac{1}{2}} \; , \; k^2 < k_{\parallel}^2 \end{cases} \quad . \quad (5.9)$$

For $\zeta(x,y) = \zeta_o e^{iQx}$ we obtain

$$\hat{\zeta}(\underline{k}_{\parallel}) = (2\pi)^2 \zeta_o \; \delta(\underline{Q} - \underline{k}_{\parallel}) \quad , \quad (5.10)$$

where

$$\underline{Q} = Q\hat{\underline{e}}_x \quad . \quad (5.11)$$

Equation (5.8) finally yields[18]

$$G_{ET}^R = \frac{E_z^R}{\mu} = -ik^3 \zeta_o(\epsilon-1) \frac{Q^2 e^{ik_2 d}}{k_1 - \epsilon k_2} \int_0^{\infty} du \; (1-R_p) \frac{u^3}{\ell_1} e^{-\ell_1 \bar{d}} \quad , \quad (5.12)$$

where k_1 and k_2 are now defined as in Eq. (5.9) with $k_{\parallel}$ replaced by Q.

Previously, we have also solved the same problem by the image method through the application of the image theory for a rough boundary, established by Rahman and Maradudin.[21] The result thus obtained can be expressed as[14]

$$G_{IT}^{R} = \frac{4\zeta_o}{\pi} \frac{\epsilon-1}{(\epsilon+1)^2} \int_0^\infty du \int_0^\infty dv \ (\epsilon fg+h)\exp[-(f+g)d] \quad , \qquad (5.13)$$

where f, g and h are functions of u and v, given by

$$f(u,v) = [(u+\tfrac{Q}{2})^2 + v^2]^{\frac{1}{2}} \quad ,$$

$$g(u,v) = [(u-\tfrac{Q}{2})^2 + v^2]^{\frac{1}{2}} \quad , \qquad (5.14)$$

$$h(u,v) = u^2 + v^2 - \frac{Q^2}{4} \quad .$$

Hence for this problem, according to Eq. (5.6), Eqs. (5.4) and (5.13) provide a complete description of A within IT, whereas Eqs. (5.5) and (5.12) provide a complete dynamical theory (ET) for A. We have carried out detailed numerical studies of these results for different metal substrates such as Ag, Au, Cu and Ni, where both ω and d were varied. For illustrative purposes, we have reproduced some results in Fig. 2. In general, we arrive at the following conclusions:[14,17,18] (i) IT can be very inaccurate for both flat and rough surfaces in the case of a highly-conducting substrate or for large molecule-surface distances; (ii) the surface-plasmon effect can cause serious damping when ω is close to the resonance frequency; (iii) surface roughness can either enhance or diminish the flat-surface value for this induced decay, depending on ω, d and the orientation of the admolecule.

Although we have most of the time considered the sinusoidal grating as a prototype of rough surfaces, other kinds of roughness have also been considered in the literature. As an example, Arias, Aravind and Metiu[13] have constructed an IT for admolecules at surfaces with randomly-distributed (Gaussian) roughness. To extend ET to this case, one has to include contributions to $E(\omega)$ which are second order in ζ,[18] since the first-order contribution will vanish in this case. Nevertheless, we expect that similar comparisons will be obtained as in Fig. 2.

VI. CONCLUSIONS

In this paper, we have summarized some of our recent results on the spectroscopic properties for atoms as well as molecules in the vicinity of a dielectric surface. For the case of adatoms near a flat surface, a fully quantum electrodynamical (QED) treatment has been followed where the atomic lifetimes, polarization of the atomic dipole and photon correlation phenomena have been analyzed. For the case of a molecular dipole in the vicinity of a rough metallic surface, a simpler classical phenomenological approach has been followed to establish a dynamical theory of the surface-induced decay rates. It is found that the hitherto available static (image) theory has very limited validity. Future directions in this research may involve a more exact QED treatment for the case of rough surfaces (along the same lines as we did for flat surfaces), as well as possible nonlinear surface spectroscopy due to a high-intensity laser field or special surface properties. To this later aspect, we have recently looked into the possibility of applying the technique of optical phase conjugation by a surface[22] to study possible novel spectroscopic phenomena for a system of molecules in the vicinity of such surfaces.

ACKNOWLEDGMENTS

REFERENCES

1. W. Jhe, A. Anderson, E. A. Hinds, D. Meschede, L. Moi and S. Haroche, Phys. Rev. Lett. 58, 666 (1987).

2. D. J. Heinzen, J. J. Childs, J. E. Thomas and M. S. Feld, Phys. Rev. Lett. 58, 1320 (1987).

3. P. W. Milonni, Phys. Rev. A. 25, 1315 (1982).

4. W. H. Louisell, Quantum Statistical Properties of Radiation (Wiley, New York, 1973).

5. H. F. Arnoldus and T. F. George, J. Chem. Phys. (1987), submitted.

6. M. R. Philpott, J. Chem. Phys. 62, 1812 (1975).

7. H. F. Arnoldus and T. F. George, Phys. Rev. A (1987), submitted.

8. G. S. Agarwal, Quantum Optics, Springer Tracts in Modern Physics, Vol. 70 (Springer, Berlin, 1974).

9. H. F. Arnoldus and T. F. George, J. Phys. B. (1987), submitted.

10. R. Rossetti and L. E. Brus, J. Chem. Phys. 73, 572 (1980); ibid. 76 1146 (1982).

11. G. E. Korzeniewski, T. Maniv and H. Metiu, J. Chem. Phys. 76, 1564 (1982).

12. R. R. Chance, A. Prock and R. Silbey, Adv. Chem. Phys. 37, 1 (1978).

13. J. Arias, P. K. Aravind and J. Metiu, Chem. Phys. Lett. 85, 404 (1982).

14. P. T. Leung, Z. C. Wu, D. A. Jelski and T. F. George, Phys. Rev. B 15, (1987), in press.

15. H. Metiu, Prog. Surf. Sci. 17, 153 (1984).

16. A. Campion, A. R. Gallo, C. B. Harris, H. J. Robota and P. M. Whitmore, Chem. Phys. Lett. 73, 447 (1980).

17. P. T. Leung, T. F. George and Y. C. Lee, J. Chem. Phys. (1987), in press.

18. P. T. Leung and T. F. George, Phys. Rev. B (1987), submitted.

19. A. A. Maradudin and D. L. Mills, Phys. Rev. B 11, 1392 (1975).

20. G. S. Agarwal, Phys. Rev. B 14, 846 (1976).

21. T. Rahman and A. A. Maradudin, Phys. Rev. B 21, 504 (1980).

19

FIGURE CAPTIONS

Fig. 1. Plot of the parallel (curve a) and perpendicular (curve b) inverse lifetimes as a function of the relative permittivity ϵ, and in the limit of a zero atom-surface distance. For $\epsilon \to -\infty$ the curves approach the values $b_{\parallel}(0) = 0$ and $b_{\perp}(0) = 2$, corresponding to a perfect conductor. We notice that $b_{\parallel}(0)$ is almost independent of ϵ and approximately equal to zero over the entire ϵ range. Only for $\epsilon \approx 0$ does it attain a finite value. From curve b we see that $b_{\perp}(0)$ gradually changes as a function of ϵ, and that it never reaches its perfect-conductor limit for any reasonable value of ϵ.

Fig. 2. Comparison between the energy transfer theory (ET, solid curves) and the image theory (IT, dotted curves) for decay rates of admolecules. Curves a and b are the values of $\text{Im}G^R$ for an Ag grating substrate ($\zeta_0 = 0.7\text{Å}$, $Q = 0.01 \text{ Å}^{-1}$) at $\omega = 2.5$ eV, and curves c and d are the values of $\text{Im}G^F$ for a flat Ni surface at $\omega = 3.3$ eV. The unit of G is Å^{-3}. The role of the substrate conductivity is evident from these graphs.

Fig. 1

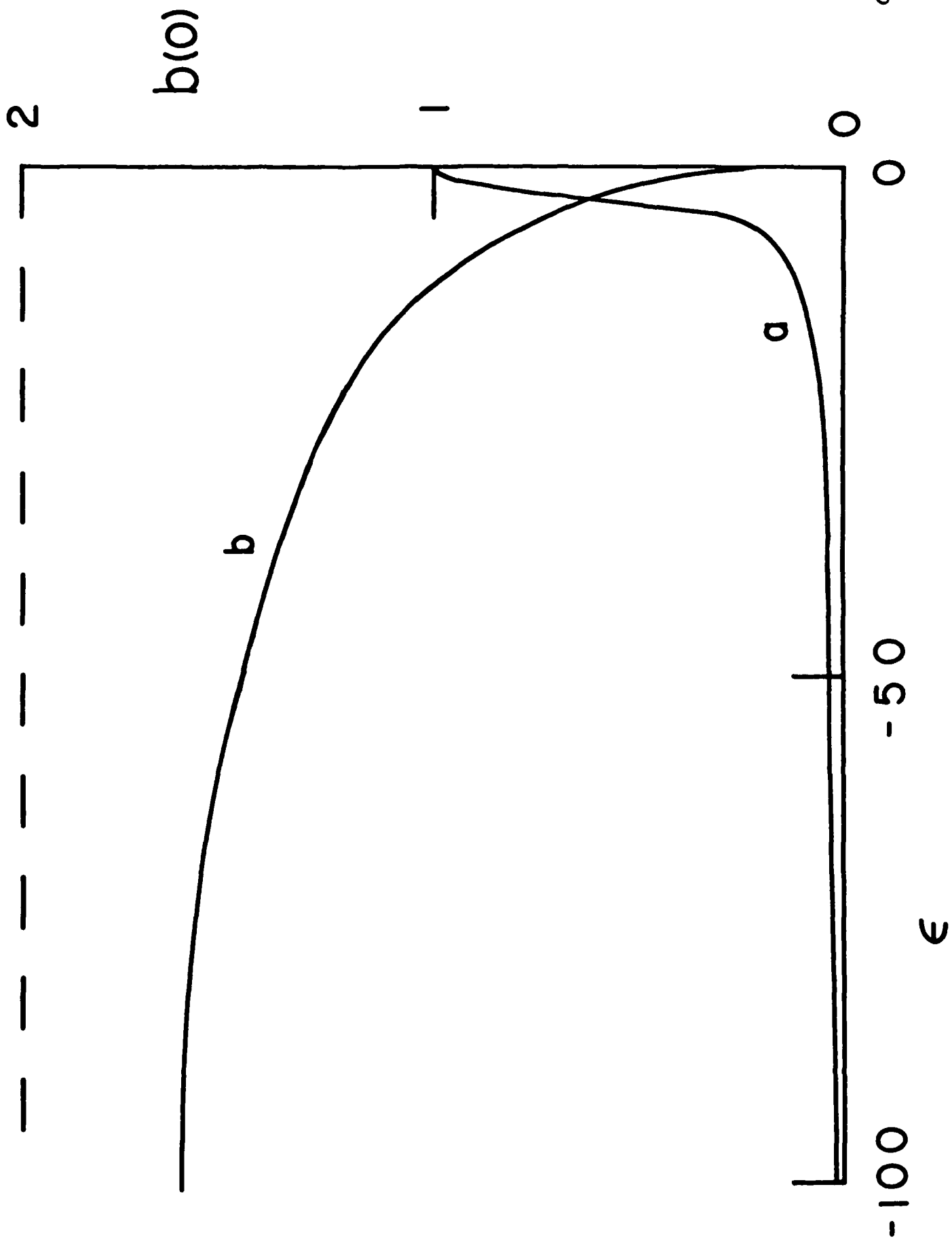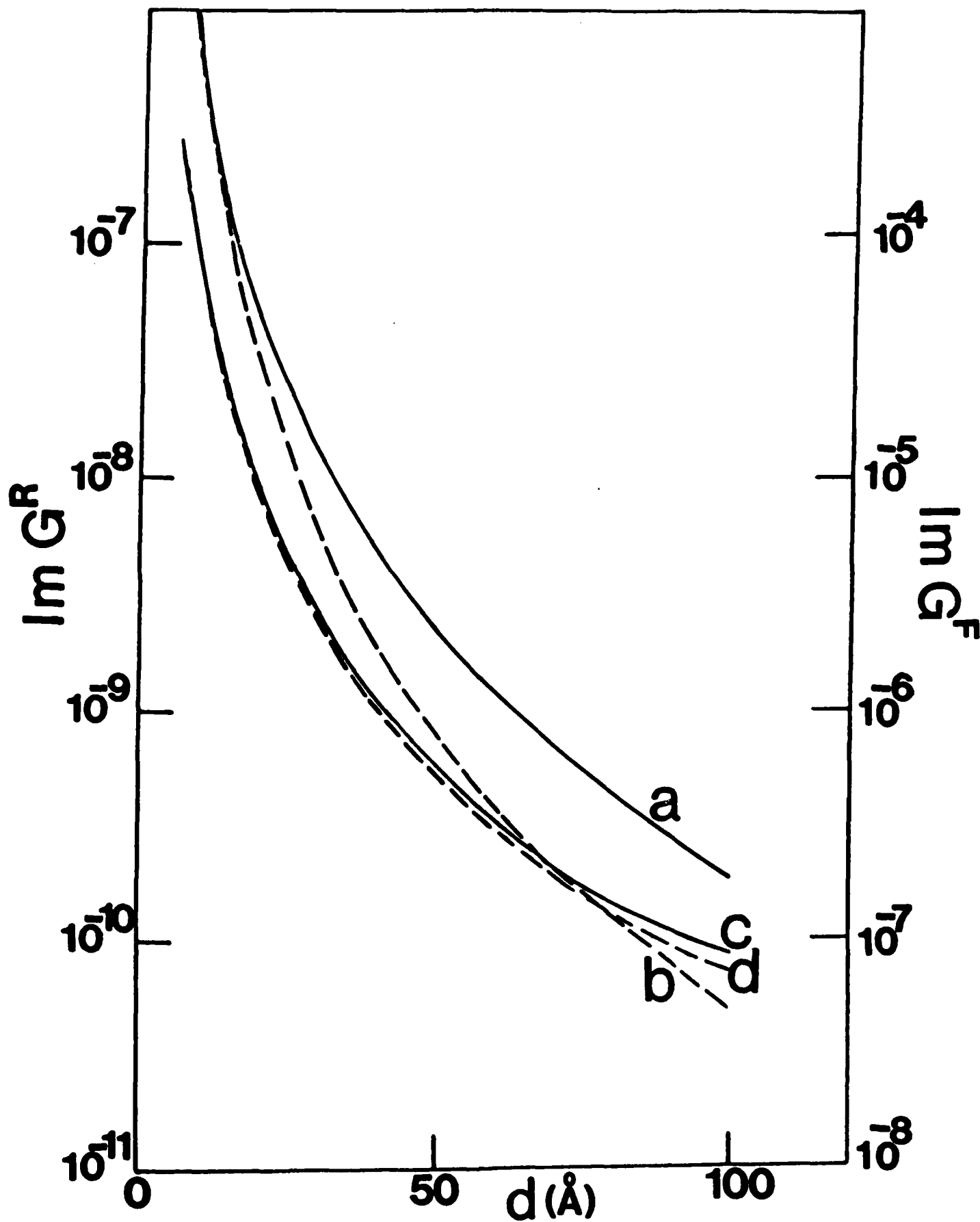Fig. 2

TECHNICAL REPORT DISTRIBUTION LIST, GEN

	No. Copies		No. Copies
Office of Naval Research Attn: Code 1113 800 N. Quincy Street Arlington, Virginia 22217-5000	2	Dr. David Young Code 334 NORDA NSTL, Mississippi 39529	1
Dr. Bernard Douda Naval Weapons Support Center Code 50C Crane, Indiana 47522-5050	1	Naval Weapons Center Attn: Dr. Ron Atkins Chemistry Division China Lake, California 93555	1
Naval Civil Engineering Laboratory Attn: Dr. R. W. Drisko, Code L52 Port Hueneme, California 93401	1	Scientific Advisor Commandant of the Marine Corps Code RD-1 Washington, D.C. 20380	1
Defense Technical Information Center Building 5, Cameron Station Alexandria, Virginia 22314	12 high quality	U.S. Army Research Office Attn: CRD-AA-IP P.O. Box 12211 Research Triangle Park, NC 27709	1
DTNSRDC Attn: Dr. H. Singerman Applied Chemistry Division Annapolis, Maryland 21401	1	Mr. John Boyle Materials Branch Naval Ship Engineering Center Philadelphia, Pennsylvania 19112	1
Dr. William Tolles Superintendent Chemistry Division, Code 6100 Naval Research Laboratory Washington, D.C. 20375-5000	1	Naval Ocean Systems Center Attn: Dr. S. Yamamoto Marine Sciences Division San Diego, California 91232	1
		Dr. David L. Nelson Chemistry Division Office of Naval Research 800 North Quincy Street Arlington, Virginia 22217	1

ABSTRACTS DISTRIBUTION LIST, 056/625/629

Dr. J. E. Jensen
Hughes Research Laboratory
3011 Malibu Canyon Road
Malibu, California 90265

Dr. J. H. Weaver
Department of Chemical Engineering
  and Materials Science
University of Minnesota
Minneapolis, Minnesota 55455

Dr. A. Reisman
Microelectronics Center of North Carolina
Research Triangle Park, North Carolina
    27709

Dr. M. Grunze
Laboratory for Surface Science and
        Technology
University of Maine
Orono, Maine 04469

Dr. J. Butler
Naval Research Laboratory
Code 6115
Washington D.C. 20375-5000

Dr. L. Interante
Chemistry Department
Rensselaer Polytechnic Institute
Troy, New York 12181

Dr. Irvin Heard
Chemistry and Physics Department
Lincoln University
Lincoln University, Pennsylvania 19352

Dr. K.J. Klaubunde
Department of Chemistry
Kansas State University
Manhattan, Kansas 66506

Dr. C. B. Harris
Department of Chemistry
University of California
Berkeley, California 94720

Dr. F. Kutzler
Department of Chemistry
Box 5055
Tennessee Technological University
Cookesville, Tennessee 38501

Dr. D. DiLella
Chemistry Department
George Washington University
Washington D.C. 20052

Dr. R. Reeves
Chemistry Department
Renssaeler Polytechnic Institute
Troy, New York 12181

Dr. Steven M. George
Stanford University
Department of Chemistry
Stanford, CA 94305

Dr. Mark Johnson
Yale University
Department of Chemistry
New Haven, CT 06511-8118

Dr. W. Knauer
Hughes Research Laboratory
3011 Malibu Canyon Road
Malibu, California 90265

ABSTRACTS DISTRIBUTION LIST, 056/625/629

Dr. G. A. Somorjai
Department of Chemistry
University of California
Berkeley, California 94720

Dr. J. Murday
Naval Research Laboratory
Code 6170
Washington, D.C. 20375-5000

Dr. J. B. Hudson
Materials Division
Rensselaer Polytechnic Institute
Troy, New York 12181

Dr. Theodore E. Madey
Surface Chemistry Section
Department of Commerce
National Bureau of Standards
Washington, D.C. 20234

Dr. J. E. Demuth
IBM Corporation
Thomas J. Watson Research Center
P.O. Box 218
Yorktown Heights, New York 10598

Dr. M. G. Lagally
Department of Metallurgical
  and Mining Engineering
University of Wisconsin
Madison, Wisconsin 53706

Dr. R. P. Van Duyne
Chemistry Department
Northwestern University
Evanston, Illinois 60637

Dr. J. M. White
Department of Chemistry
University of Texas
Austin, Texas 78712

Dr. D. E. Harrison
Department of Physics
Naval Postgraduate School
Monterey, California 93940

Dr. R. L. Park
Director, Center of Materials
  Research
University of Maryland
College Park, Maryland 20742

Dr. W. T. Peria
Electrical Engineering Department
University of Minnesota
Minneapolis, Minnesota 55455

Dr. Keith H. Johnson
Department of Metallurgy and
  Materials Science
Massachusetts Institute of Technology
Cambridge, Massachusetts 02139

Dr. S. Sibener
Department of Chemistry
James Franck Institute
5640 Ellis Avenue
Chicago, Illinois 60637

Dr. Arnold Green
Quantum Surface Dynamics Branch
Code 3817
Naval Weapons Center
China Lake, California 93555

Dr. A. Wold
Department of Chemistry
Brown University
Providence, Rhode Island 02912

Dr. S. L. Bernasek
Department of Chemistry
Princeton University
Princeton, New Jersey 08544

Dr. W. Kohn
Department of Physics
University of California, San Diego
La Jolla, California 92037

7

ABSTRACTS DISTRIBUTION LIST, 056/625/629

Dr. F. Carter
Code 6170
Naval Research Laboratory
Washington, D.C. 20375-5000

Dr. Richard Colton
Code 6170
Naval Research Laboratory
Washington, D.C. 20375-5000

Dr. Dan Pierce
National Bureau of Standards
Optical Physics Division
Washington, D.C. 20234

Dr. R. Stanley Williams
Department of Chemistry
University of California
Los Angeles, California 90024

Dr. R. P. Messmer
Materials Characterization Lab.
General Electric Company
Schenectady, New York 22217

Dr. Robert Gomer
Department of Chemistry
James Franck Institute
5640 Ellis Avenue
Chicago, Illinois 60637

Dr. Ronald Lee
R301
Naval Surface Weapons Center
White Oak
Silver Spring, Maryland 20910

Dr. Paul Schoen
Code 6190
Naval Research Laboratory
Washington, D.C. 20375-5000

Dr. John T. Yates
Department of Chemistry
University of Pittsburgh
Pittsburgh, Pennsylvania 15260

Dr. Richard Greene
Code 5230
Naval Research Laboratory
Washington, D.C. 20375-5000

Dr. L. Kesmodel
Department of Physics
Indiana University
Bloomington, Indiana 47403

Dr. K. C. Janda
University of Pittsburg
Chemistry Building
Pittsburg, PA 15260

Dr. E. A. Irene
Department of Chemistry
University of North Carolina
Chapel Hill, North Carolina 27514

Dr. Adam Heller
Bell Laboratories
Murray Hill, New Jersey 07974

Dr. Martin Fleischmann
Department of Chemistry
University of Southampton
Southampton 509 5NH
UNITED KINGDOM

Dr. H. Tachikawa
Chemistry Department
Jackson State University
Jackson, Mississippi 39217

Dr. John W. Wilkins
Cornell University
Laboratory of Atomic and
  Solid State Physics
Ithaca, New York 14853

ABSTRACTS DISTRIBUTION LIST, 056/625/629

Dr. R. G. Wallis
Department of Physics
University of California
Irvine, California 92664

Dr. D. Ramaker
Chemistry Department
George Washington University
Washington, D.C. 20052

Dr. J. C. Hemminger .
Chemistry Department
University of California
Irvine, California 92717

Dr. T. F. George
Chemistry Department
University of Rochester
Rochester, New York 14627

Dr. G. Rubloff
IBM
Thomas J. Watson Research Center
P.O. Box 218
Yorktown Heights, New York 10598

Dr. Horia Metiu
Chemistry Department
University of California
Santa Barbara, California 93106

Dr. W. Goddard
Department of Chemistry and Chemical
    Engineering
California Institute of Technology
Pasadena, California 91125

Dr. P. Hansma
Department of Physics
University of California
Santa Barbara, California 93106

Dr. J. Baldeschwieler
Department of Chemistry and
    Chemical Engineering
California Institute of Technology
Pasadena, California 91125

Dr. J. T. Keiser
Department of Chemistry
University of Richmond
Richmond, Virginia 23173

Dr. R. W. Plummer
Department of Physics
University of Pennsylvania
Philadelphia, Pennsylvania 19104

Dr. E. Yeager
Department of Chemistry
Case Western Reserve University
Cleveland, Ohio 41106

Dr. N. Winograd
Department of Chemistry
Pennsylvania State University
University Park, Pennsylvania 16802

Dr. Roald Hoffmann
Department of Chemistry
Cornell University
Ithaca, New York 14853

Dr. A. Steckl
Department of Electrical and
    Systems Engineering
Rensselaer Polytechnic Institute
Troy, NewYork 12181

Dr. G.H. Morrison
Department of Chemistry
Cornell University
Ithaca, New York 14853

END

7-87

DTIC